Supporting Information:

Electrochemical Phase Engineering of Li-Ti-P-O Nanocomposite Thin Films

Daniela R. Fontecha*[1], Osma Gomez[3], Nam Soo Kim[4], Sang Bok Lee[1, 3, 4], Gary W. Rubloff[1,2], Keith E. Gregorczyk*[1]

[1]Department of Materials Science and Engineering at University of Maryland, College Park, MD, 20742, USA

[2]Institute for Systems Research at University of Maryland, College Park, MD, 20742, USA

[3]Department of Chemistry and Biochemistry, University of Maryland, College Park, MD, 20742, USA

[4]Maryland NanoCenter, Institute for Research in Electronics and Applied Physics, University of Maryland, College Park, MD, 20742, USA

Corresponding Authors:

Keith E. Gregorczyk: kgregorc@umd.edu

Daniela R. Fontecha: drfontec@umd.edu

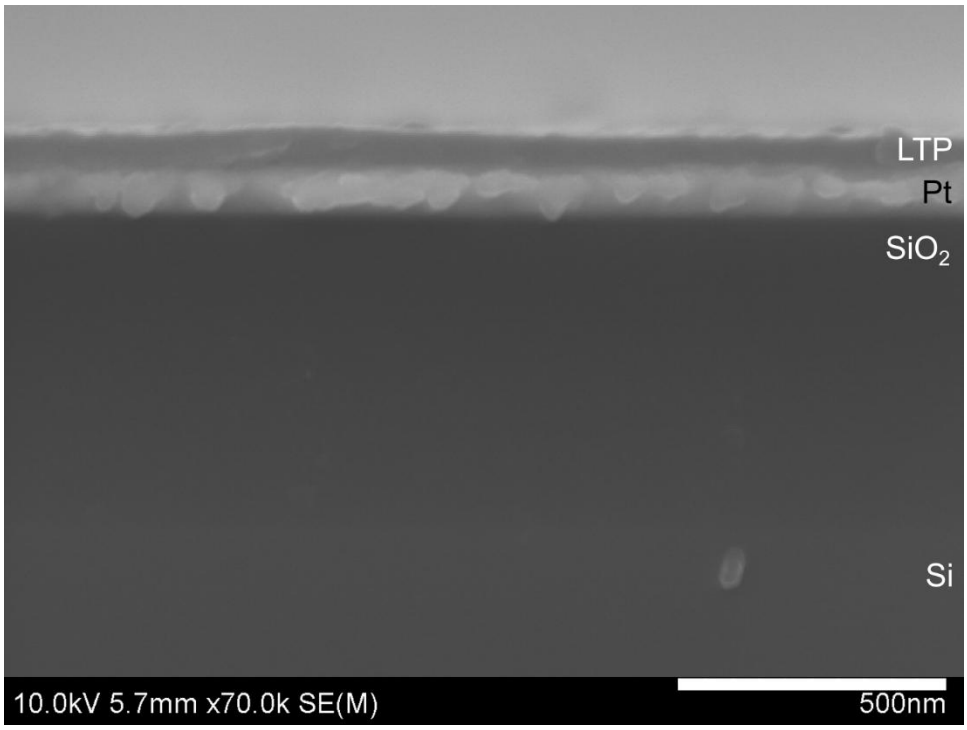

S1. SEM cross section of an LTP film (60 ± 2 nm) on Pt (100 nm, nominal) and SiO2 (500 nm, nominal) on a Si test wafer.

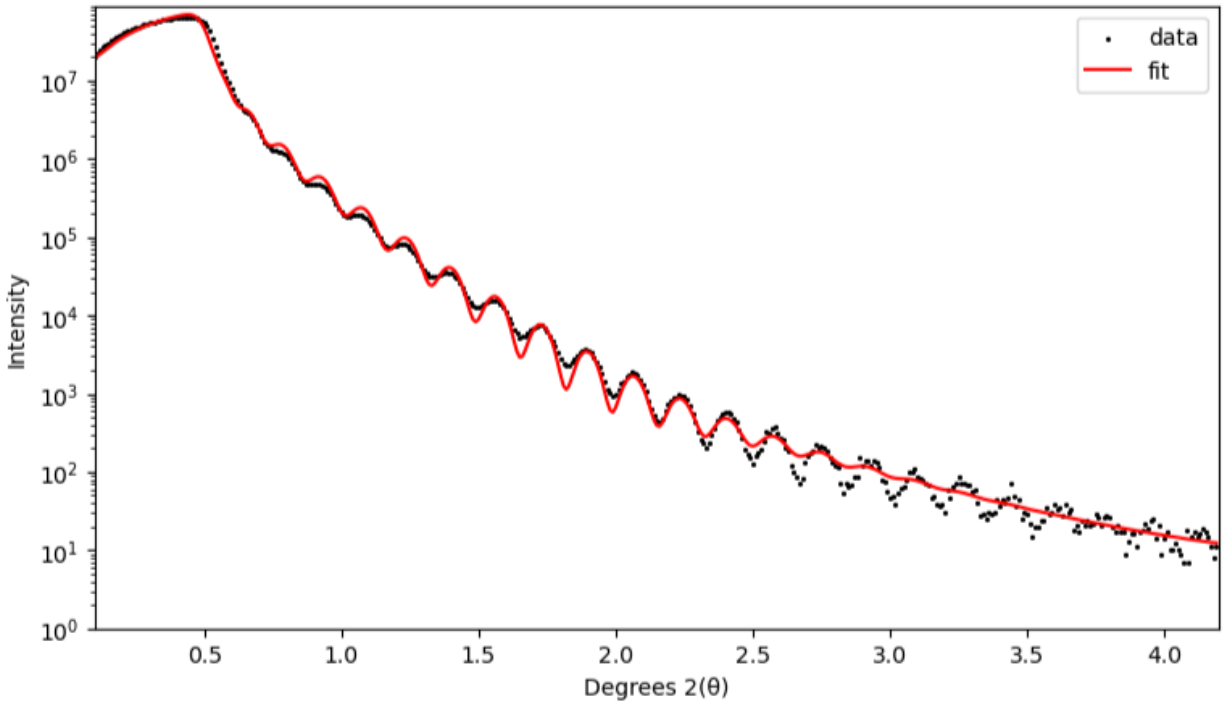

S2. X-ray reflectometry raw spectrum was fitted with GenX software to measure film density (2.9 g/cm^3). This value was then used in concurrence with the film thickness (60 ± 2 nm) and exposed sample area (0.631 ± 0.002 cm^2 for beaker cell measurements or 0.283 ± 0.002 cm^2 for T-cell measurements) to calculate the mass of the active material in the electrochemical measurements.

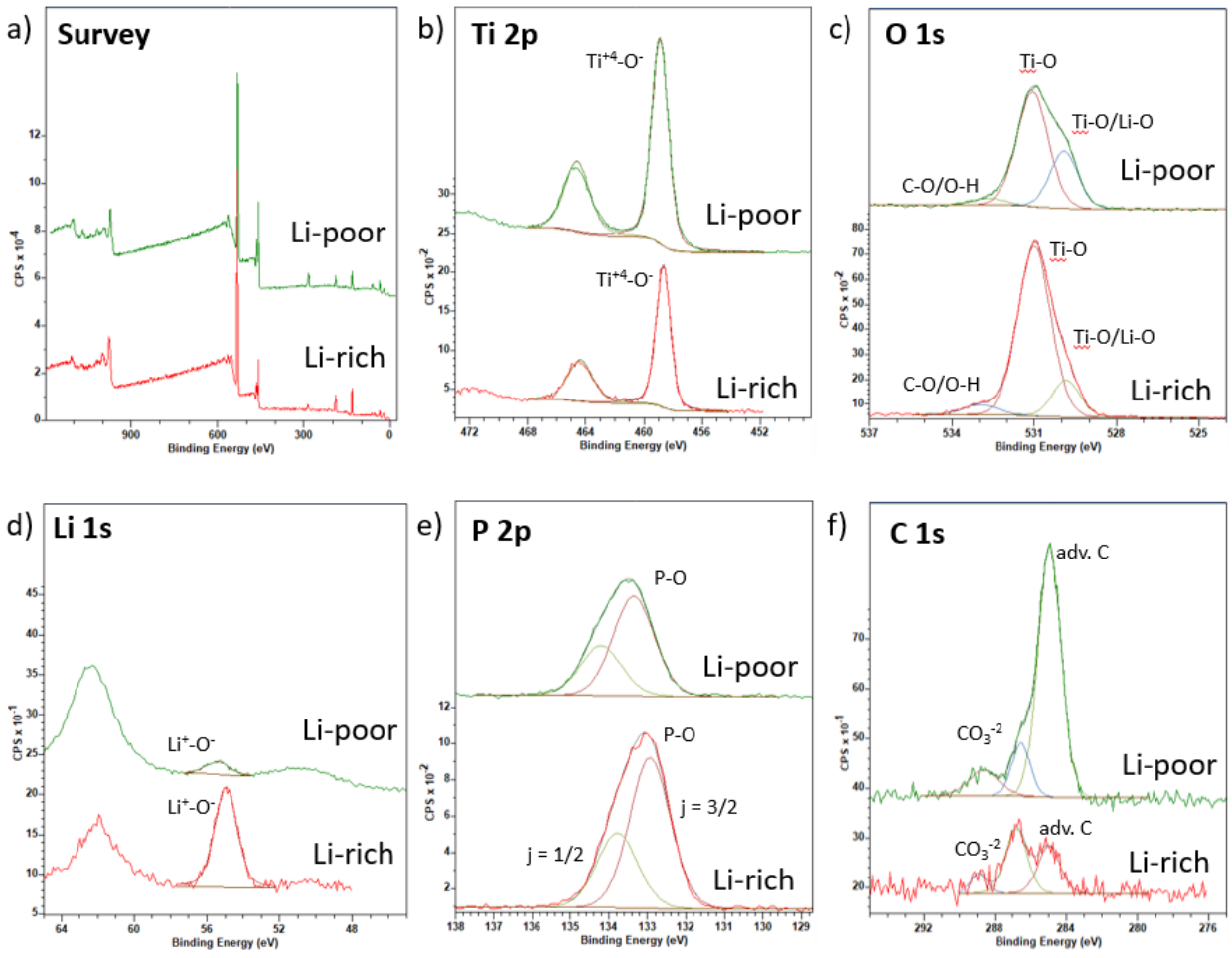

S3. X-ray photoelectron spectroscopy of Li-rich and Li-poor as-deposited ALD films. a) survey spectrum. b-f) high resolution spectra of Ti 2p, O 1s, Li 1s, P 2p, and C 1s, respectively.

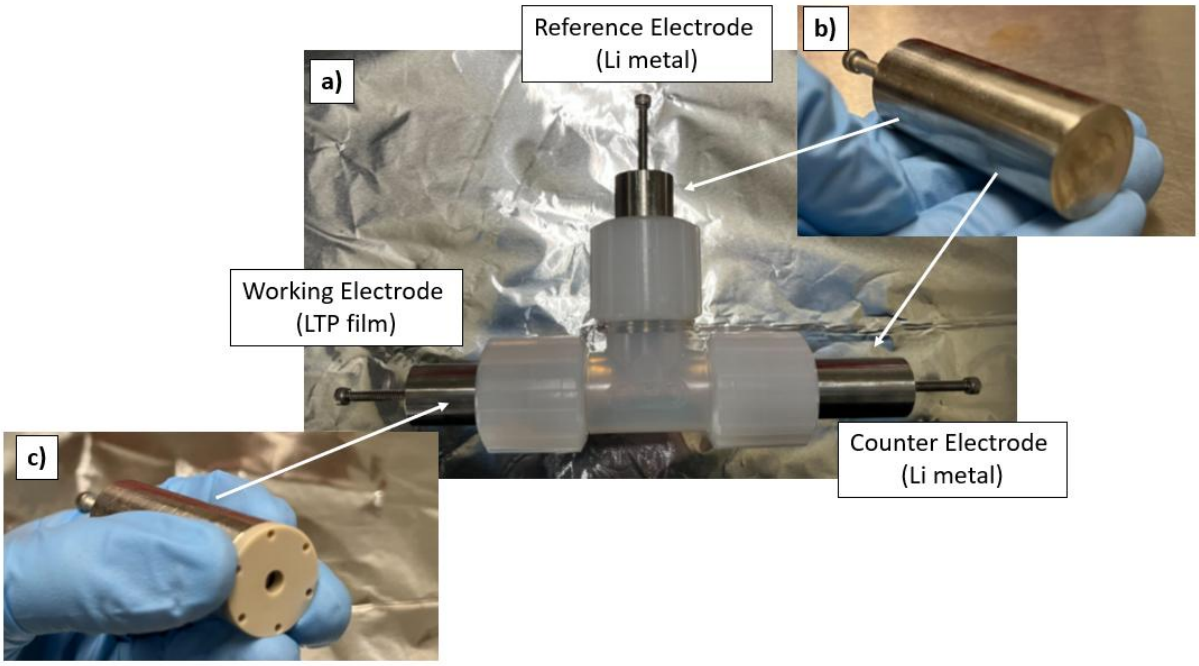

S4. Image a) shows the three electrode T-cell configuration used for data in **Figures 7 and 8** of the main text. b) The reference and counter electrodes are stainless steel rods where a round piece of lithium foil was pressed against the flat side to make good contact with the rod and placed inside the respective places in the T-cell. c) The working electrode was made by modifying the stainless steel rod such that a 1x1 cm^2 Si chip with the SiO2/Pt/LTP stack could be inserted on the face of the rod, then held in place by an insulating plate (PEEK). In between the sample and the insulating plate sits a silicone gasket that was used to prevent electrolyte from contacting the backside of the Si chip and to control the active area (0.283 ± 0.002 cm^2).

Figure Number	Voltage Window (V vs Li^+/Li)	C-rate	Current Density (A/ng)	Gravimetric capacity (mAh/g)	Areal capacity (uAh/cm^2)	Volumetric capacity (mAh/cm^3)
6	1.6 - 3.5 V	1	0.3	317 (10.8)	5.5 (0.02)	919.3 (31.3)
		2	0.6	300 (10.2)	5.2 (0.02)	870 (29.6)
		4	1.1	280 (9.6)	4.9 (0.02)	814.9 (27.8)
		10	2.9	250 (8.5)	4.4 (0.01)	725 (24.7)
		20	5.7	220 (7.5)	3.8 (0.01)	640.9 (21.8)
7	0.5 - 3.5 V	1	1.2	1305 (45.2)	22.7 (0.2)	3784.5 (131.0)
		2	2.4	1171 (36.6)	20.4 (0.1)	3395.9 (117.6)
		4	4.9	1056 (36.6)	18.4 (0.1)	3062.4 (106.0)
		10	12.2	917 (31.8)	16.0 (0.1)	2659.3 (92.1)
		20	23.8	807 (27.9)	14.0 (0.1)	2340.3 (81.0)
8 (with crystalline LTP)	2.1 - 3.5 V	1	0.1	125 (4.3)	2.2 (0.02)	362.5 (12.6)
		2	0.2	116 (4.0)	2.0 (0.01)	336.4 (11.6)
		4	0.4	107 (3.7)	1.9 (0.01)	310.3 (10.7)
		10	1	98 (3.4)	1.7 (0.01)	284.2 (9.8)
		20	1.9	91 (3.2)	1.6 (0.01)	263.9 (9.1)
		50	4.8	83 (2.9)	1.4 (0.01)	240.7 (8.3)
		100	9.5	79 (2.7)	1.4 (0.01)	229.1 (7.9)
		150	14.3	76 (2.6)	1.3 (0.01)	220.4 (7.6)

		200	19.1	74 (2.6)	1.3 (0.01)	214.6 (7.4)
8 (without crystalline LTP)	2.1 - 3.5 V	1	0.1	143 (5.0)	2.5 (0.01)	414.7 (14.4)
		2	0.2	101 (3.5)	1.8 (0.01)	292.9 (10.1)
		4	0.4	80 (2.8)	1.4 (0.01)	232 (8.0)
		10	1	64 (2.2)	1.1 (0.01)	185.6 (6.4)
		20	1.9	54 (1.9)	0.9 (0.01)	156.6 (5.4)
		50	4.8	43 (1.5)	0.7 (0.01)	124.7 (4.3)
		100	9.5	35 (1.2)	0.6 (0.004)	101.5 (3.5)
		150	14.3	30 (1.0)	0.5 (0.004)	87 (3.0)
		200	19.1	27 (0.9)	0.5 (0.003)	78.3 (2.7)

S5. Table of the gravimetric current densities used in the galvanostatic charge/discharge curves of Li-poor LTP nanocomposites at different C-rates for each voltage window reported in the manuscript. Included are also the gravimetric, areal, and volumetric capacities reported in this work for the corresponding figures. The errors are reported in parentheses in the same units as the respective value on the table.

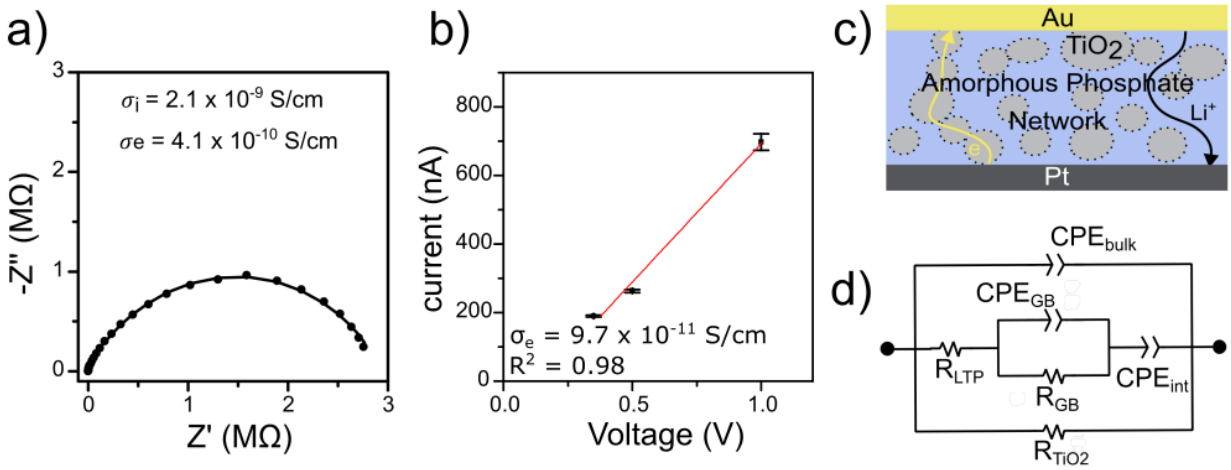

S6. From Fontecha et al (Copyright by Daniela Rosa Fontecha Solano 2025).[1] Impedance results of the Pt/LTP/Au metal-insulator-metal stack of a) Nyquist plot from EIS and b) DC relaxation data. c) Physical representation of ionic and electronic behavior in the LTP (n = 2) as-deposited film and d) corresponding equivalent electric circuit used to fit the Nyquist plot in (a). In this equivalent circuit model, constant phase elements (CPEs) are used to represent imperfect capacitances in the material. $CPE_{interface,}$ and CPE_{bulk} represent capacities at the film/metal interface and the bulk of the film, respectively. R_{TiO2} represents the electronic conduction through TiO_2 domains. R_{LTP} represents Li^+ ion conduction through the lithium titanium phosphate. The electronic conductivity resulting from the equivalent circuit model fit is 4.1 x 10^{-10} S/cm, in agreement with the DC relaxation measurements in (b), showing an electronic conductivity of 9.7 x 10^{-11} S/cm.

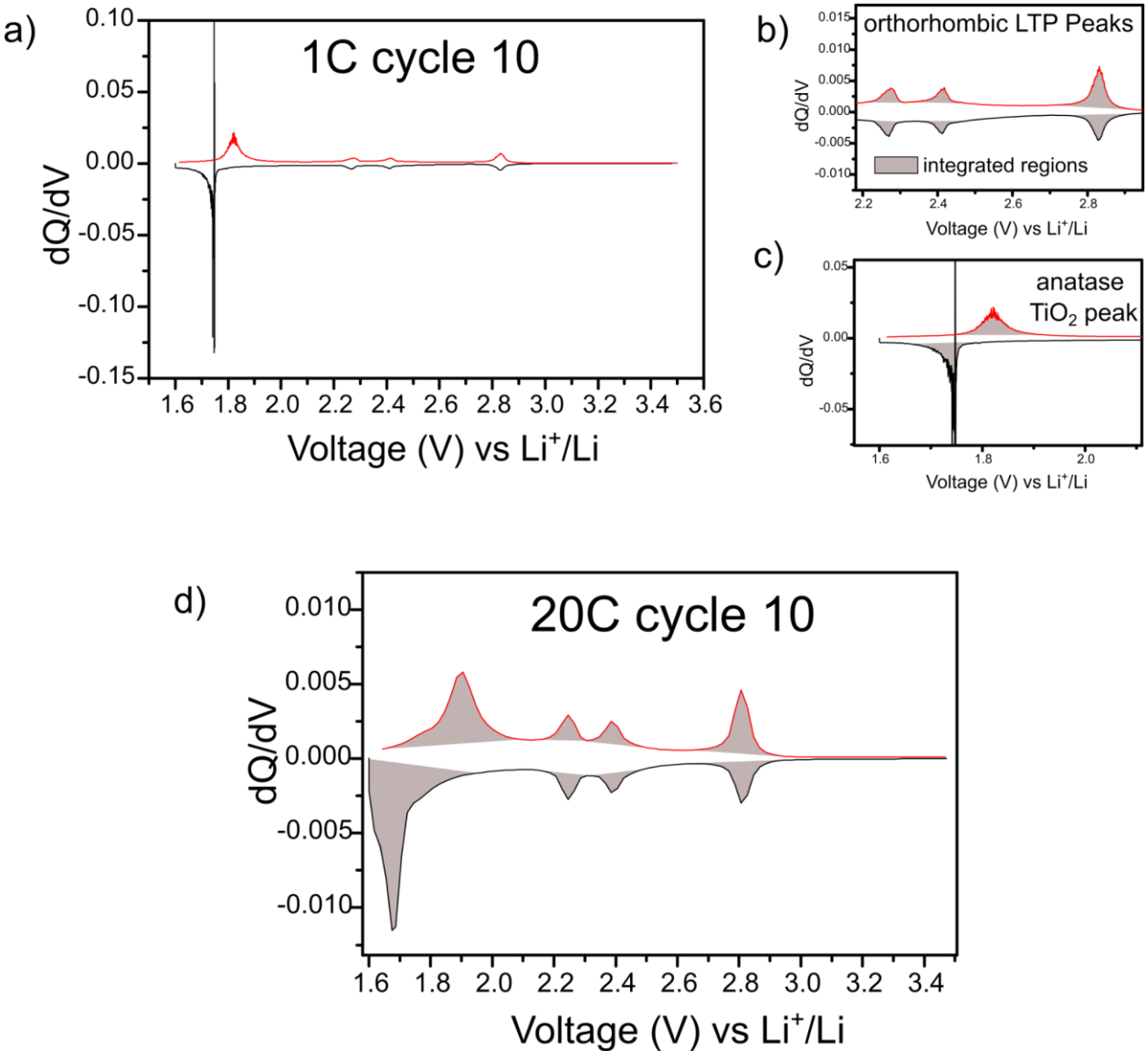

S7. The capacity contributions from each phase were estimated by integrating the redox region of the dQ/dV from the rate tests in **Figure 6** of the manuscript, using a straight line baseline to generate the integration area. a) shows the dQ/dV of LTP (n = 2) cycled at 1C between 1.2 V – 3.5 V vs Li^+/Li. Zoomed in versions of b) the orthorhombic LTP peaks and c) the TiO_2 peaks are displayed with the gray region corresponding to the integration area used for the capacity calculations of the respective components at 1C. The total capacity was calculated by using zero as the baseline to subtract from the redox capacities to estimate changes in the amorphous matrix capacity. d) shows the same analysis performed on the sample cycled at 20 C.

Charging rate	***Peak position (V vs Li^+/Li)***	***Charge Capacity (mAh/g)***
1C	2.8	27.5 (0.9)
	2.45	10.9 (0.4)
	2.25	10.2 (0.3)
	1.82	99.2 (3.4)
20C	2.8	27.9 (1.0)
	2.45	9.3 (0.3)
	2.25	8.9 (0.3)
	1.8	62.5 (2.1)

S8. Table of the results from the integration in S7 at each cycling rate (1C and 20C) with the integrated charge capacity for each oxidation peak. Calculated errors are included in parentheses in mAh/g.

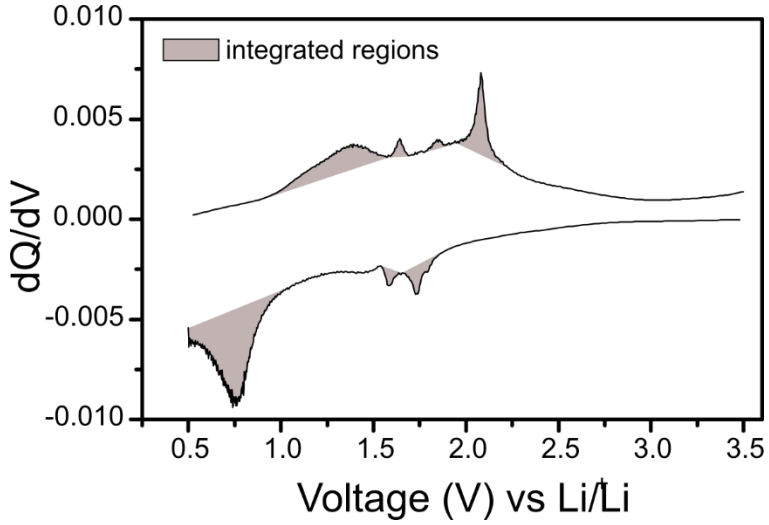

S9. The figure shows the integration regions of the redox peaks of the dQ/dV at 1C from 0.5 V – 3.5 V vs Li^+/Li of an annealed LTP nanocomposite where the orthorhombic grains were electrochemically removed. The integrated regions in gray of the redox peaks were subtracted from the total capacity to arrive at the pseudocapacitance contribution to the capacity in this sample. In this case, the redox peaks on discharge contribute 216 ± 7.5 mAh/g, the total discharge capacity is 1305.9 ± 45.2 mAh/g, leaving 1090 ± 37.7 mAh/g as pseudocapacitive contribution. On the charge, the redox peaks contribute 180 ± 6.2 mAh/g while the total capacity is 1266 ± 43.8 mAh/g, leaving 1086 ± 37.6 mAh/g as pseudocapacitive contribution.

S10. Explanation of the calculation for estimating the amorphous matrix capacity for the Li-poor LTP film cycled from 0.5 V - 3.5 V vs Li^+/Li in **Figure 7**.

Step 1 - Assumptions:

In the Li-poor annealed sample before cycling there are three distinct phases - anatase TiO_2, orthorhombic LTP, and *amorphous* LTP (as seen in Scheme 1b of the manuscript). After cycling down to < 0.5 V vs Li^+/Li, the crystalline LTP phase vitrifies due to a high degree of lithiation (Scheme 1c). This phenomenon is supported by **Figures 4 and 5** in the manuscript and by literature.[2,3] For the purposes of the capacity that is measured, we can think of the crystalline LTP being consumed by the amorphous LTP phase, so now a larger percentage of the film is composed of amorphous LTP and the only crystalline phase is anatase TiO_2.

To know if a total capacity of 1302 mAh/g is reasonable, we need to try to estimate the amount of each phase present and assign their respective capacities. The theoretical capacities for lithiated crystalline LTP ($Li_3Ti_2(PO_4)_3$) and lithium titanate ($LiTiO_2$) are 133.5 mAh/g and 335.5 mAh/g, respectively. However, we don't have a good way to estimate the theoretical capacity of the amorphous matrix because of challenges present in measuring the film structural composition of

this complex semicrystalline system. Estimating the amount of each phase present before electrochemical vitrification is not trivial but we have made the effort to estimate these values with a combination of structural XRD data and electrochemical data detailed below.

Step 2 - Deconvolution of phase fractions:

In our previous work we quantified the ratio of NASICON LTP and anatase TiO_2 crystallites by Rietvelt refinement for the *Li-rich* nanocomposite, resulting in a breakdown of 44.8 wt. % NASICON and 55.2 wt. % anatase.[4] However, this did not indicate how much of the film is actually amorphous vs crystalline, which is a very important parameter to know in order to be able to calculate the specific capacities of each individual phase. Calculating the amorphous phase weight percent with XRD and Reitvelt refinement requires control samples in the fully amorphous and fully crystalline regimes, which is not practical for us to realize in this case. Additionally, the 1302 mAh/g and all other rate tests in this work were performed on the *Li-poor* film which grew orthorhombic LTP rather than NASICON LTP grains. Unfortunately, this is one of the lesser studied polymorphs of the $Li_{1+x}Ti_2(PO_4)_3$ family, making it difficult to perform Rietvelt refinement on this particular composition.

Since we could not source any structural files for the pbca orthorhombic LTP structure in the common databases (ICSD and COD) to perform the Rietvelt refinement, we instead performed a spectrum matching analysis with Diffrac.EVA software. We matched reference diffractograms of anatase TiO_2 and pbca Fe-doped LTP (the closest match in the database) to our Li-poor nanocomposite sample. These results are shown in **S11** below. According to the wt. % calculation from this closest match on Diffrac.EVA, the crystalline portion of the film can best be estimated to be composed of ~67 wt. % orthorhombic LTP and ~33 wt. % anatase TiO_2. Given that this is not a perfect method, we can take these two results (the Diffrac.EVA calculation for Li-poor sample and Rietvelt refinement for Li-rich sample) and propose that we could have somewhere between **~45-67 wt. % orthorhombic LTP** in the crystalline part of the Li-poor sample. Although this is a wide range, it at least gives us upper and lower bounds to carry on our capacity calculations.

That takes care of the relative amount of crystalline phases present but still does not address how much of the film is amorphous vs crystalline. One way to *estimate* the weight percent of crystalline content is from galvanostatic voltammetry results. At a rate approaching equilibrium (0.1 C, 0.56 uA/cm^2) cycling between 1.6 V to 3.5 V vs Li^+/Li, one can calculate the capacitive contribution to each phase (relative to the total film mass) and compare this to the corresponding theoretical capacities of anatase TiO_2 and orthorhombic LTP. From here we can use this information to arrive at an estimate of the relative weight percent of each phase. The contribution to the total capacity coming from each redox peak was isolated by integrating the area under the dQ/dV peaks (excluding the pseudocapacitive background) (see **S7b-c** for more details on the integration method). **S12** summarizes these calculations in which the relative fractions of each phase present were estimated as follows: 22.8 % orthorhombic LTP, 28.1 % anatase TiO2, and 49.1 % amorphous matrix. These results align well with the Rietvelt refinement of our previous work that indicated a near 50/50 split between the NASICON and anatase crystalline phases in weight percent.[4] If we also consider the

spectrum matching results for orthorhombic LTP, this gives us a range of ~23 - 34 wt. % orthorhombic LTP of the total film.

Step 3 - Calculations of amorphous phase capacity:

Now, looking at the capacity of the vitrified sample that was cycled down to 0.5 V as in **Figure 7b**, the removal of the orthorhombic LTP phase means that an additional 23 - 31 wt. % of the film is amorphous LTP, totaling ~72 - 83 wt % amorphous LTP. For a sample cycled down to 0.5 V vs Li^+/Li at a charging rate of 1C, a total film gravimetric capacity of 1302 mAh/g (assuming a theoretical capacity of anatase to be 333.5 mAh/g) corresponds to **~1500 - 1679 mAh/g** for the amorphous LTP phase.

While this is a high capacity, and some assumptions have been made to be able to get to an estimate, this estimated amorphous matrix capacity falls within the range of similar amorphous metal phosphates reported in literature.[5] Amorphous metal phosphates (e.g., $V_2O_5 \bullet P_2O_5$, $SnO_2 \bullet P_2O_5$) have been extensively studied as anode materials and have shown to be able to accommodate a large amount of lithium in their amorphous phosphate networks (ranging from 500 - 1650 mAh/g), especially at lower potentials where the transition metal oxide becomes highly reduced.[6] Some work on the $V_2O_5 \bullet P_2O_5$ system has also demonstrated that nanostructuring the glass anodes with embedded electronic conductors like reduced graphene oxide (rGO) plays an important role in increasing the coulombic efficiency of the first cycle, showing a ~66 % increase in stable capacity in $75V_2O_5 \bullet 25P_2O_5$ coated with rGO on particle diameters on the order of microns.[7] Our LTP system takes this approach to the nanoscale in which both the film thickness (60 nm) and the electronic conductor (TiO2, 5-40 nm diameter) operate at very small feature sizes. This provides plenty of pathways for Li^+ insertion and extraction and reduces diffusion limitations in the system as suggested by Kebede et. al., that could result in much higher capacity retention.

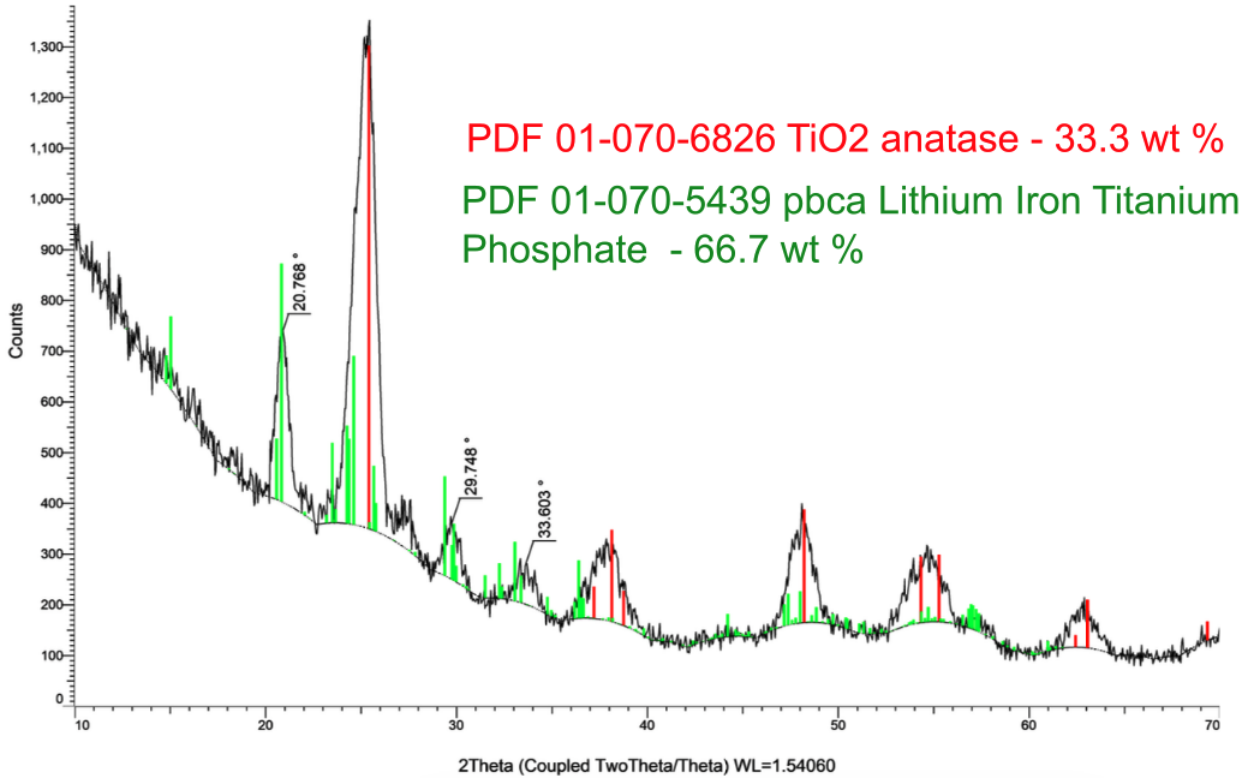

S11. Diffrac.EVA spectrum matching results with the acquired GI-XRD spectrum of the Li-poor LTP film (black). The red peaks correspond to reference anatase TiO_2 (PDF 01-070-6826) and the green peaks correspond to lithium iron titanium phosphate (pace group pbca, PDF 01-070-5439).

Phase of Redox Peaks	**Integrated Capacity (mAh/g) of total film mass**	**Theoretical Capacity (mAh/g)**	**Weight Percent in Film (%)**
Othorhombic LTP Phase	31.5	138	22.8
Anatase TiO_2 Phase	94.5	336	28.1

S12. Calculation of Weight Percent of orthorhombic and Anatase Crystalline Phases in ALD Semicrystalline Nanocomposite.

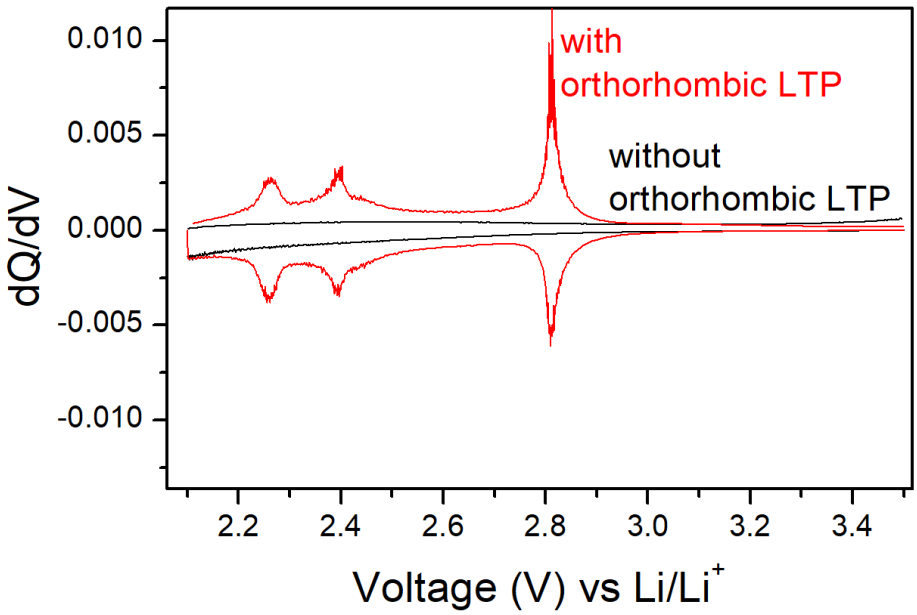

S13. dQ/dV of LTP samples with and without orthorhombic LTP cycled at 1C. Samples with orthorhombic LTP were cycled in a beaker cell (0.61 ± 0.002 cm^2 exposed area) while samples without orthorhombic LTP were cycled in a T-cell (0.283 ± 0.002 cm^2 exposed area), to avoid reaction of Si on the side wall of the substrate with the liquid electrolyte at the low voltages required to remove the orthorhombic LTP phase.

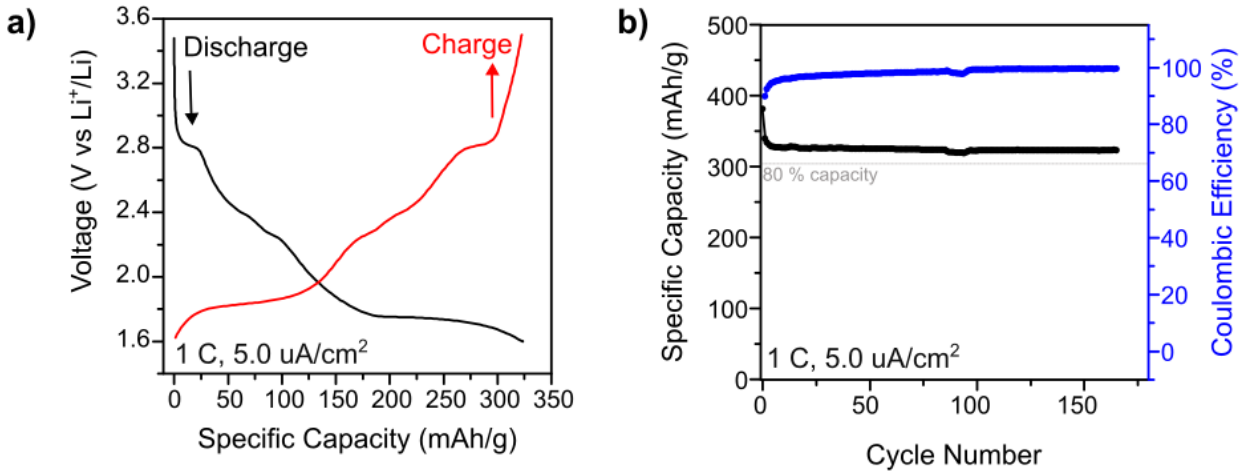

S14. Electrochemical cycling results of Li-poor films annealed at 650 °C for 8.5 min in the voltage window where orthorhombic LTP and TiO_2 are both redox active in a beaker cell vs Li^+/Li. a) Galvanostatic charge-discharge curves of the first cycle, and c) capacity retention curves over 140 cycles between 1.6 V to 3.5 V vs Li^+/Li. The plateaus in the charge and discharge profiles in **S14a** match the redox peaks present in the cyclic voltammogram in **Figure 2** in the manuscript and show a total capacity of 323 ± 11.2 mAh/g. **S14b** shows the cycling stability of the LTP/TiO_2

nanocomposite at a charging rate of 1 C. Though the capacity initially drops in the first forming cycle, the coulombic efficiency stabilizes at 99.6 % with a final capacity of 274 ± 9.5 mAh/g in the 166th cycle.

References

(1) Fontecha, D. R. Tuning the Ionic and Electronic Properties of Metal Phosphates by Atomic Layer Deposition. *Digit. Repos. Univ. Md.* **2025**. https://doi.org/https://doi.org/10.13016/ano9-oebr.

(2) Srout, M.; Lasri, K.; Dahbi, M.; Kara, A.; Tetard, L.; Saadoune, I. Understanding of the Li-Insertion Process in a Phosphate Based Electrode Material for Lithium Ion Batteries. *J. Power Sources* **2019**, *435*, 226803. https://doi.org/10.1016/j.jpowsour.2019.226803.

(3) Wang, G. X.; Bradhurst, D. H.; Dou, S. X.; Liu, H. K. LiTi2(PO4)3 with NASICON-Type Structure as Lithium-Storage Materials. *J. Power Sources* **2003**, *124* (1), 231–236. https://doi.org/10.1016/S0378-7753(03)00609-8.

(4) Fontecha, D. R.; Kozen, A. C.; Stewart, D. M.; Hall, A. T.; Cumings, J.; Rubloff, G. W.; Gregorczyk, K. E. Nanoscale Mixed Ion-Electron-Conducting NASICON-Type Thin Films: Lithium Titanium Phosphate via Atomic Layer Deposition. *ACS Appl. Mater. Interfaces* **2025**, *17* (17), 25358–25369. https://doi.org/10.1021/acsami.5c02201.

(5) Yu, L.; Zhao, S.-X.; Wu, X.; Li, J.-W.; Zhao, E.-L.; Wei, G.-D. Lithium Ion Storage Behaviors of (100-x) V2O5-(x) P2O5 Glass as Novel Anode Materials for Lithium Ion Battery. *J. Alloys Compd.* **2019**, *810*, 151938. https://doi.org/10.1016/j.jallcom.2019.151938.

(6) Shang, C.; Li, X.; Wei, R.; Liu, X.; Xu, S.; Zhang, J. Research Progress of Metal Oxide Glass Anode Materials for Lithium-Ion Batteries: A Review. *J. Non-Cryst. Solids* **2023**, *618*, 122547. https://doi.org/10.1016/j.jnoncrysol.2023.122547.

(7) Kebede, M. A.; Palaniyandy, N.; Ramadan, R. M.; Sheha, E. The Electrical and Electrochemical Properties of Graphene Nanoplatelets Modified 75V2O5–25P2O5 Glass as a Promising Anode Material for Lithium Ion Battery. *J. Alloys Compd.* **2018**, *735*, 445–453. https://doi.org/10.1016/j.jallcom.2017.11.136.